Article

Cell

Circadian Rhythms in Rho1 Activity Regulate Neuronal Plasticity and Network Hierarchy

Graphical Abstract

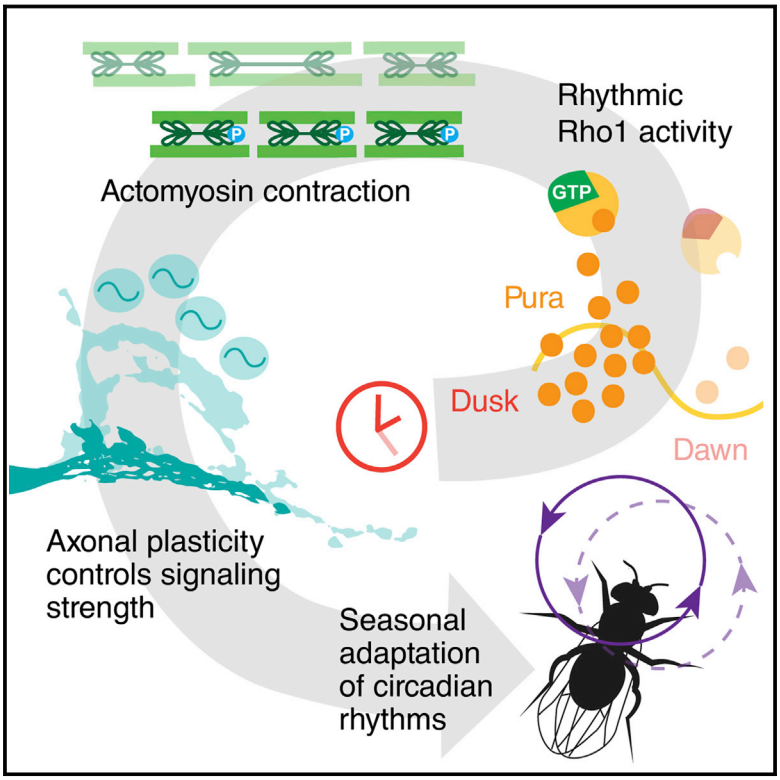

Authors

Afroditi Petsakou, Themistoklis P. Sapsis, Justin Blau

Correspondence

justin.blau@nyu.edu

In Brief

24-hr oscillations in Rho1 activity in *Drosophila* pacemaker neurons drive rhythms in the structure of their axonal projections and in the abundance of synaptic markers. This plasticity is required to change hierarchy within the clock neural network to allow flies to adapt to different seasons.

Highlights

- Clock-regulated expression of *Pura* leads to circadian rhythms in Rho1 activity
- Rhythmic Rho1 activity drives structural and synaptic plasticity in pacemaker neurons
- Rho1-induced plasticity in LNv pacemaker neurons modulates their signaling
- LNv plasticity alters clock network hierarchy for seasonal adaptation and rhythmicity

Petsakou et al., 2015, Cell *162*, 1–13
August 13, 2015
http://dx.doi.org/10.1016/j.cell.2015.07.010

CellPress

Please cite this article in press as: Petsakou et al., Circadian Rhythms in Rho1 Activity Regulate Neuronal Plasticity and Network Hierarchy, Cell (2015), http://dx.doi.org/10.1016/j.cell.2015.07.010

Article

Cell

Circadian Rhythms in Rho1 Activity Regulate Neuronal Plasticity and Network Hierarchy

Afroditi Petsakou,[1,6] Themistoklis P. Sapsis,[2,3] and Justin Blau[1,4,5,*]
[1]Department of Biology, New York University, 100 Washington Square East, New York, NY 10003, USA
[2]Courant Institute for Applied Mathematics, New York University, New York, NY 10003, USA
[3]Department of Mechanical Engineering, Massachusetts Institute of Technology, Cambridge, MA 02142, USA
[4]Center for Genomics & Systems Biology, New York University Abu Dhabi, Abu Dhabi, United Arab Emirates
[5]Program in Biology, New York University Abu Dhabi, Abu Dhabi, United Arab Emirates
[6]Present address: Department of Genetics, Harvard Medical School, Boston, MA 02115, USA
*Correspondence: justin.blau@nyu.edu
http://dx.doi.org/10.1016/j.cell.2015.07.010

SUMMARY

Neuronal plasticity helps animals learn from their environment. However, it is challenging to link specific changes in defined neurons to altered behavior. Here, we focus on circadian rhythms in the structure of the principal s-LNv clock neurons in *Drosophila*. By quantifying neuronal architecture, we observed that s-LNv structural plasticity changes the amount of axonal material in addition to cycles of fasciculation and defasciculation. We found that this is controlled by rhythmic Rho1 activity that retracts s-LNv axonal termini by increasing myosin phosphorylation and simultaneously changes the balance of pre-synaptic and dendritic markers. This plasticity is required to change clock network hierarchy and allow seasonal adaptation. Rhythms in Rho1 activity are controlled by clock-regulated transcription of *Puratrophin-1-like* (*Pura*), a Rho1 GEF. Since spinocerebellar ataxia is associated with mutations in human *Puratrophin-1*, our data support the idea that defective actin-related plasticity underlies this ataxia.

INTRODUCTION

A plastic nervous system allows organisms to adapt to and learn from their environment. Although many neurons in the brain show plasticity, there are relatively few examples where structural changes in defined adult neurons are understood at the molecular level and have clear-cut behavioral consequences. This is due to difficulties in identifying and manipulating the precise neurons whose structure has changed in a densely packed brain during adulthood (May, 2011). Structural plasticity is thus often studied in vitro (Matsuzaki et al., 2004).

Almost all organisms have circadian rhythms of behavior and disturbances to human circadian rhythms can result in psychiatric disorders (Zelinski et al., 2014). Circadian rhythms are controlled by pacemaker neurons in the brain. These neurons receive external signals such as light to synchronize behavior with the solar day, although circadian rhythms persist in constant darkness (DD). A set of clock genes form a molecular clock that drives 24-hr oscillations in RNA and protein levels in clock neurons. In *Drosophila*, this clock is composed of the transcriptional activators Clock (CLK) and Cycle (CYC), which activate the clock genes *period* (*per*) and *timeless* (*tim*). After translation, PER and TIM enter the nucleus, where PER represses CLK/CYC to close the negative feedback loop. Similar genes act in a conserved manner in the mammalian clock (reviewed by Yu and Hardin, 2006). Additional clock-controlled genes such as K^+ channels that change firing properties of clock neurons help transduce molecular clock time into rhythmic electrical activity (Meredith et al., 2006; Ruben et al., 2012).

In addition to rhythms in intrinsic excitability, the structure of both *Drosophila* s-LNvs and mammalian pacemaker neurons is remodeled daily, and, at least in s-LNvs, this is clock-controlled (Becquet et al., 2008; Fernández et al., 2008; Girardet et al., 2010). However, the behavioral correlates of circadian structural plasticity have not yet been identified. The importance of s-LNvs in circadian behavior (Renn et al., 1999; Stoleru et al., 2004) offers an unusual opportunity to connect structural plasticity to behavior.

s-LNv axonal termini are normally maximally spread at dawn, which coincides with their peak excitability (Cao and Nitabach, 2008; Cao et al., 2013; Fernández et al., 2008). Although it was recently reported that daily changes in s-LNv termini are a cycle of fasciculation and defasciculation (Sivachenko et al., 2013), we found that s-LNvs add and lose axonal material with a 24-hr rhythm.

We speculated that actin rearrangements drive s-LNv growth and retraction and, therefore, that Rho family GTPases (Rho, Rac, and Cdc42) are involved. GTPases act as switches that are active when bound to GTP and inactive when GDP-bound. Guanine nucleotide exchange factors (GEFs) increase GTPase activity while GTPase-activating proteins (GAPs) decrease activity (Van Aelst and D'Souza-Schorey, 1997). Rho GTPases are important in neuronal development: Rac1 and Cdc42 promote axonal elongation and branching, while RhoA (Rho1 in *Drosophila*) promotes axonal retraction (Gonzalez-Billault et al., 2012; Hall, 2012).

We found that transiently overexpressing wild-type Rho1 keeps s-LNv termini in a dusk-like retracted state and can also

Please cite this article in press as: Petsakou et al., Circadian Rhythms in Rho1 Activity Regulate Neuronal Plasticity and Network Hierarchy, Cell (2015), http://dx.doi.org/10.1016/j.cell.2015.07.010

override electrical activity-dependent expansion. We discovered that endogenous Rho1 activity shows circadian rhythms in s-LNvs that retract their axonal termini at dusk via actin contraction and myosin light-chain phosphorylation. Rho1 activity is regulated by clock-controlled expression of a previously uncharacterized GEF, which we named Puratrophin-1-like (Pura). Pura and Rho1 also orchestrate daily antiphase rhythms in pre-synaptic and dendritic markers in s-LNv termini and modulate signaling. Finally, we showed that Rho1-regulated plasticity in s-LNv termini is required for normal circadian rhythms and controls hierarchy in the clock neuronal network so that flies can adapt to different seasons. *Pura* is an ortholog of human *Puratrophin-1*, mutations of which are associated with spinocerebellar ataxia (Ishikawa et al., 2005). Our data support the idea that Puratrophin-1-related spinocerebellar ataxia is a disease of defective actin-mediated neuronal plasticity.

RESULTS

s-LNv Projections Increase Axonal Volume at Dawn

The approaches previously used to quantify the termini of s-LNv projections detected clear time of day differences (Fernández et al., 2008; Sivachenko et al., 2013). However, these methods are laborious and limited to two dimensions. They therefore cannot calculate the overall axonal volume and determine whether spreading and retraction change the total amount of axonal material. To address this, we created a MATLAB script to automatically reconstruct 3D projections from confocal stacks of s-LNv termini.

To test the script, we reconstructed s-LNv projections from flies fixed at dusk (ZT12) and dawn (ZT24) (ZT = Zeitgeber time, time in a 12:12-light:dark cycle). We used two different markers to test reproducibility: a membrane-tethered GFP expressed in LNvs using the *Pdf-Gal4* driver; and the Pigment Dispersing Factor (PDF) neuropeptide, which is required for circadian behavior and has higher levels at dawn than dusk (Park et al., 2000; Renn et al., 1999).

The 3D reconstructions and quantification in Figures 1A and S1B show that s-LNv projections are significantly less spread in each axis at ZT12 than ZT24. This makes the 3D spread of both GFP and PDF at ZT12 ~50% of the spread at ZT24 (Figure 1A). Axonal volume is also significantly reduced at ZT12 compared to ZT24 (Figure 1A), and this is independent of fluorescence levels (Figure S1B). These data indicate that axonal growth and contraction takes place simultaneously with fasciculation and defasciculation and that together these constitute the daily expansion and retraction cycles of s-LNv termini.

Rho GTPases Dynamically Regulate Adult s-LNv Structure

Given that axonal volume changes between dawn and dusk, we hypothesized that an actin-related pathway underlies s-LNv plasticity and tested whether Rho GTPases are involved. Since Rho GTPases affect neuronal development (Gonzalez-Billault et al., 2012), we restricted overexpression to adulthood (Figure 1B). We used *tubulin-Gal80^{ts}* (McGuire et al., 2003) to repress *Pdf-Gal4* activity and raised flies at 19°C when Gal80^{ts} is functional. After entraining to LD cycles at 19°C, Rho GTPase expression was induced in s-LNvs by raising the temperature to 30°C to inactivate Gal80^{ts}. We induced expression of Rho1, Rac1, or Cdc42 for 12 hr starting at dusk (ZT12). Brains were dissected, fixed, and stained at ZT24* (asterisk indicates prior 12 hr of induction), when s-LNvs are normally maximally spread (Fernández et al., 2008).

We found that inducing wild-type Rho1 significantly reduced the 3D spread of s-LNv projections to ~50% of the 3D spread of control projections at ZT24* (Figure 1B). Inducing constitutively active Cdc42 or wild-type Rac1 had the opposite effect (Figures 1B and S1D). Rac1 increased the spread of s-LNv projections in the x and y axes, while Cdc42^{CA} increased the spread in x and y axes but reduced z axis spread (Figures 1B and S1D). The rapid response of s-LNv projections to Rho GTPase induction suggests they normally play a role in s-LNv expansion and retraction.

Sivachenko et al. (2013) proposed that the transcription factor Mef2 regulates expression of the inter-cellular adhesion molecule Fas2 as a mechanism for s-LNv plasticity. However, we found that inducing *Fas2* for 12 hr did not significantly change the spread in the x or y axes, the 3D spread or the axonal volume, although the z axis spread was reduced (Figure S1E). Given these limited effects of *Fas2* induction, some of the defects detected by Sivachenko et al. (2013) may be due to continuous *Fas2* overexpression during development and early adulthood.

Sivachenko et al. (2013) also found that s-LNv projections can change rapidly. They increased LNv electrical activity at dusk using the heat-sensitive ion channel TrpA1 and found that s-LNv projections expand to a dawn-like state within 2 hr. This requires the transcription factor Mef2. We tested whether inducing Rho1 can also affect activity-dependent spreading of s-LNvs. We found that a 3-hr shift from 19°C to 30°C starting at ZT12 induces sufficient TrpA1 expression and activity to increase the 3D spread and axonal volume of s-LNvs to a dawn-like state (Figures 1C and S1F). This expansion was blocked by simultaneously inducing Rho1 (Figure 1C). Thus, Rho1 can regulate s-LNv plasticity in a highly dynamic manner, and the similar phenotypes of *Mef2^{RNAi}* (Sivachenko et al., 2013) and Rho1 (Figure 1C) suggest they are in the same pathway.

Rho1-Induction Locks s-LNv Projections in a Dusk-like State

We decided to focus on Rho1 since it was the only Rho GTPase to block the expansion of s-LNvs (Figures 1B and S1D). We next tested whether inducing Rho1 expression can reduce s-LNv projections at any time of day. Rho1 was induced starting either at dusk (ZT12) or dawn (ZT24) with projections assayed 12 hr later. Figure 2 shows that the 3D spread and axonal volume of s-LNv projections with Rho1 induced are no different to control s-LNv projections fixed at dusk (ZT12*, Figure 2). Thus, inducing Rho1 has no effect on s-LNv projections at dusk but only affects s-LNv projections at dawn.

To test how well *tubulin-Gal80^{ts}* represses Rho1 activity, we raised flies at 19°C and shifted them to 25°C, when Gal80^{ts} is still functional (McGuire et al., 2003). Flies with control or Rho1 transgenes had strong rhythms in the 3D spread and axonal volume of s-LNv projections at 25°C (Figure S2). Thus, we conclude that *tubulin-Gal80^{ts}* represses Rho1 activity at 25°C and lower.

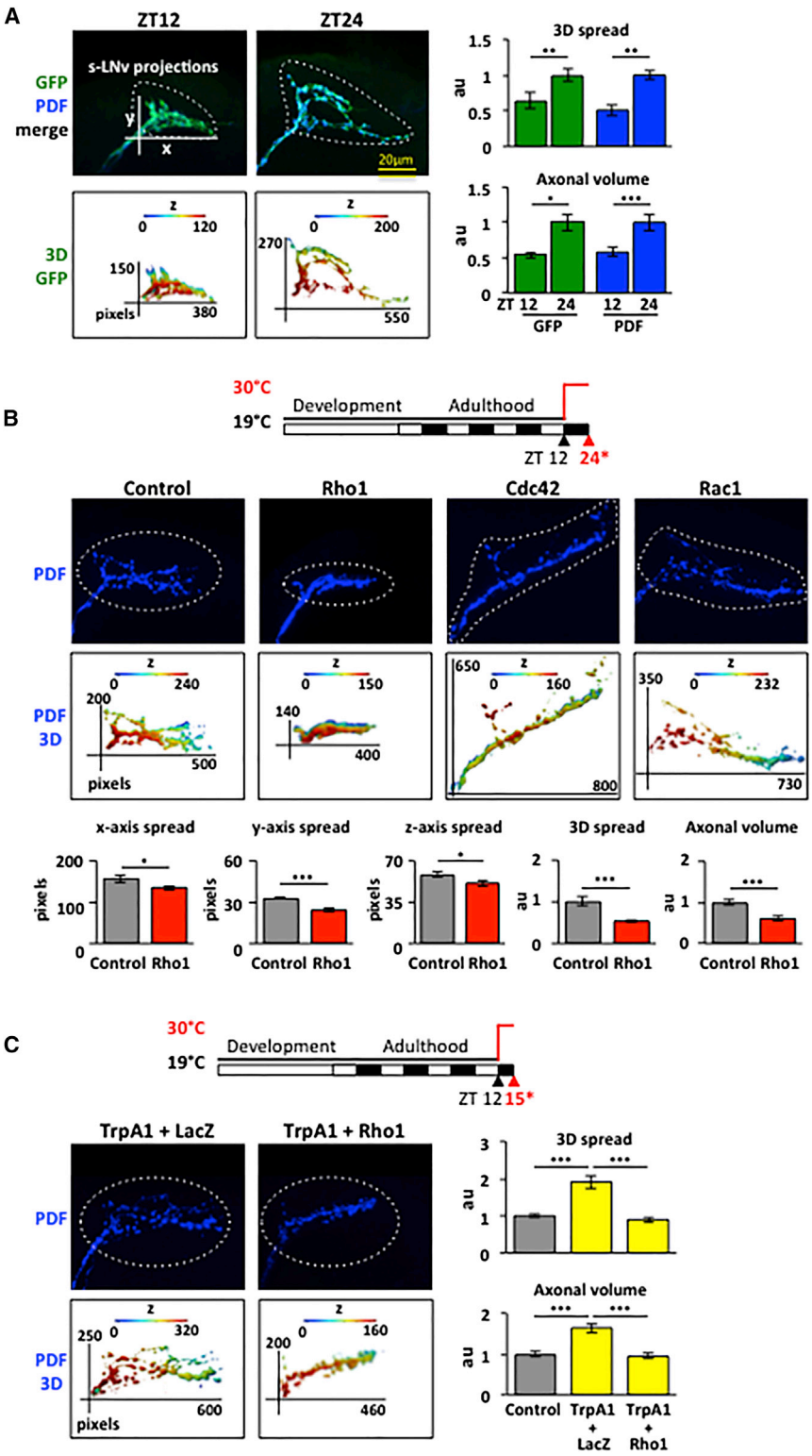

Figure 1. Rho1 Prevents s-LNv Projections from Expanding

(A) Confocal images of s-LNv projections from *Pdf > CD8::GFP* flies stained with antibodies to GFP (green) and PDF (blue) at ZT12 and ZT24. 3D reconstructions (rainbow images) were generated using the MATLAB script (see Experimental Procedures) with colors indicating depth in the z axis (blue to red represents posterior to anterior). White dots show the area quantified. 1 pixel = 0.12 μm and z-step is 1 μm. Graphs on right quantify 3D spread and axonal volume using the MATLAB script.

(B) Top: induction of Rho GTPase transgenes. Flies were raised at 19°C and entrained in LD cycles at 19°C for at least 3 days before shifting to 30°C at ZT12. Flies were dissected 12 hr later (ZT24*) and stained with anti-PDF. Confocal images of s-LNv projections and their 3D reconstructions as above at ZT24* for Control (*Pdf, tub-Gal80^{ts} > CD8::GFP*), Rho1 (*Pdf, tub-Gal80^{ts} > Rho1*), Cdc42 (*Pdf, tub-Gal80^{ts} > Cdc42^{CA}*) and Rac1 (*Pdf, tub-Gal80^{ts} > Rac1*). Graphs quantify parameters of s-LNv projections from control and Rho1-induced flies.

(C) Top: diagram of induction. Flies were handled and stained as in Figure 1B except dissection was at ZT15*. Confocal images and 3D reconstructions as above for TrpA1 + LacZ (*Pdf, tub-Gal80^{ts} > TrpA1, LacZ*) and TrpA1 + Rho1 (*Pdf, tub-Gal80^{ts} > TrpA1, Rho1*). Control flies were *Pdf, tub-Gal80^{ts} > myrRFP*. Graphs quantify s-LNv projections.

Error bars show SEM. Statistical comparisons are with Student's t test. *p < 0.05, **p < 0.01, ***p < 0.001. Significance was also verified with ANOVA. (See also Figure S1.)

Next, we measured the effect of reducing Rho1 activity using a dominant-negative Rho1 transgene (Rho1^{DN}). Figure 2 shows that the 3D spread of s-LNv projections expressing Rho1^{DN} at ZT12* is significantly higher than in control flies, indicating that s-LNv projections need maximal Rho1 activity to fully retract. However, there are still oscillations in the 3D spread and axonal volume between ZT12* and ZT24* in Rho1^{DN}-expressing s-LNvs (Figure 2). This suggests that either 12 hr of Rho1^{DN} induction does not completely eliminate Rho1 activity and/or that additional factors drive s-LNv expansion. We favor the latter idea since inducing other Rho GTPases increases s-LNv expansion at dawn (Figures 1B and S1D).

Circadian Oscillations in Endogenous Rho1 Activity in s-LNv Axons

One explanation for the time-specific effect of Rho1 induction is that endogenous Rho1 activity is rhythmic. Thus, overexpressing Rho1 would affect s-LNv projections only when endogenous Rho1 activity is low. To test this, we used a Rho1-specific activity sensor that has three Rho1-GTP binding domains fused to eGFP (Simões et al., 2006). Sensor

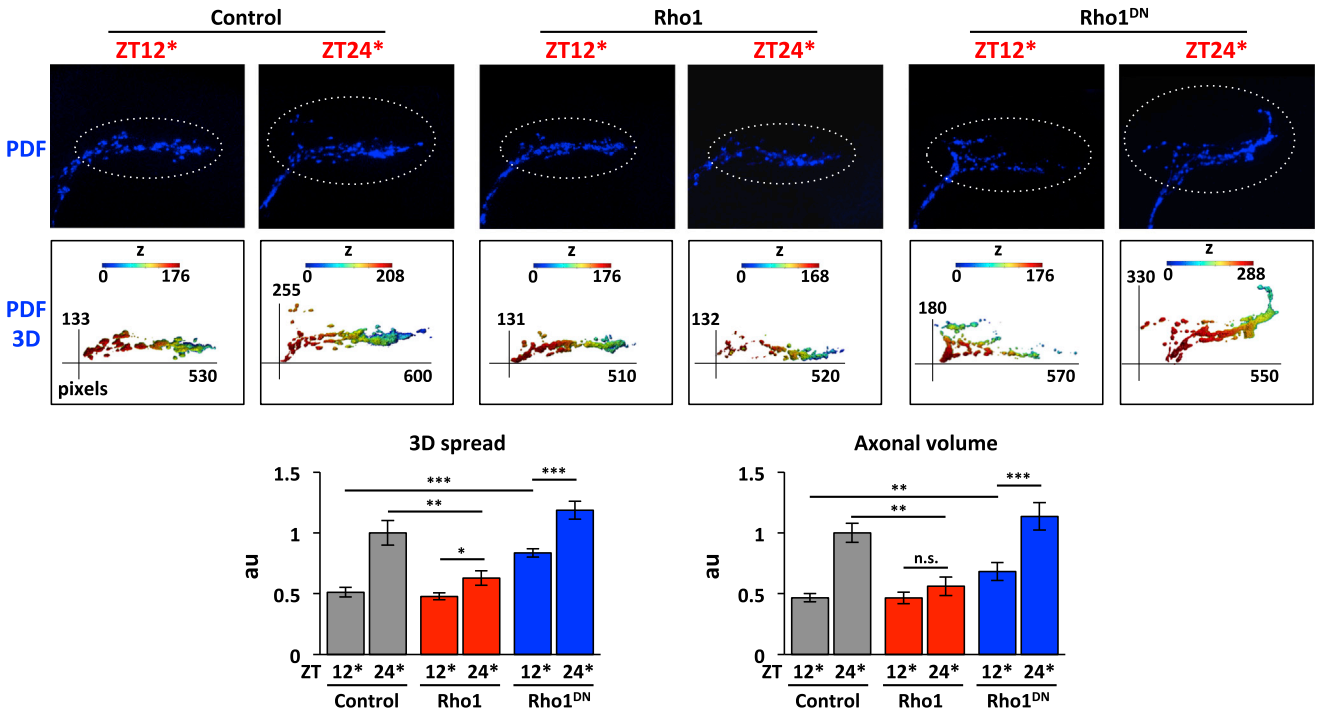

Figure 2. Inducing Rho1 Locks s-LNv Projections in a Dusk-like State

Flies were raised and entrained as in Figure 1B. Rho1 was induced starting either at dawn with brains fixed at ZT12* or starting at dusk with brains fixed at ZT24*. Confocal images of s-LNv projections and their 3D reconstructions as in Figure 1 from control (*Pdf, tub-Gal80^{ts} > myrGFP + myrRFP*), Rho1 (*Pdf, tub-Gal80^{ts} > Rho1 + myrRFP*), and Rho1^{DN} flies (*Pdf, tub-Gal80^{ts} > Rho1^{DN}*). s-LNv projections were stained with anti-PDF and quantified as in Figure 1B. 1 pixel = 0.12 μm and z-step is 1 μm. Error bars show SEM. Statistical comparisons are with Student's t test. *p < 0.05, **p < 0.01, ***p < 0.001; n.s., non-significant. Significance was also verified with ANOVA. (See also Figure S2.)

fluorescence is diffuse in the cytoplasm until endogenous Rho1 activation concentrates the sensor at the membrane to give intense fluorescence (Simões et al., 2006).

We expressed the sensor in s-LNvs, fixed fly brains at different times of day, and used a GFP antibody to quantify Rho1 activity. The data in Figure 3A show that endogenous Rho1 activity in s-LNv axons is highest around dusk. We detected oscillations in s-LNv axonal termini and the straight portion of the s-LNv axons below their ramifications (Figure 3A) but not in s-LNv cell bodies (Figure 3B). We found no rhythms in cytosolic GFP or membrane-bound RFP (Figure 3A), indicating that Rho1 sensor rhythms are not due to altered s-LNv morphology.

Next, we measured sensor activity in DD to test whether Rho1 rhythms are circadian. We found that Rho1 activity was higher at CT12 than CT24 (Figure 3C), in phase with LD rhythms. Rho1 activity rhythms in LD and DD made it likely that these oscillations are clock dependent, like s-LNv plasticity itself (Fernández et al., 2008). To test this, we assayed Rho1 sensor levels in *per^0* mutant flies. We found that Rho1-activity oscillations were lost in *per^0* mutants (Figure 3C), indicating that endogenous Rho1 activity rhythms are normally clock controlled.

Rho1 Regulates an Output Pathway Important for Circadian Behavior

We next assayed the behavioral consequences of altered s-LNv plasticity by comparing the locomotor activity of control (*Pdf, tub-Gal80^{ts} > myrRFP*) and Rho1-induced flies (*Pdf, tub-Gal80^{ts} > Rho1*). Flies were grown at 19°C, and their behavioral rhythms assayed in DD at 25°C and 30°C. Flies of both genotypes had similarly strong circadian rhythms at 25°C when Gal80^{ts} is active (Figure 4A; Table S1). However, flies with Rho1 induced by shifting to 30°C were either arrhythmic or weakly rhythmic (Figure 4A; Table S1). We confirmed that maintaining flies at 30°C keeps s-LNv projections in a dusk-like retracted state at CT24* even 2.5 days after inducing Rho1 (data not shown).

The arrhythmicity in *Pdf, tub-Gal80^{ts} > Rho1* flies could be associated with defects in the s-LNv molecular clock and/or s-LNv signaling. To test the first possibility, we measured levels of the core clock proteins TIM and Vrille (VRI) on day 3 in DD at 30°C. We found that VRI and TIM protein oscillations were indistinguishable when comparing s-LNvs in control and Rho1-induced flies (Figures 4B and S3A). Thus, the cause of arrhythmic behavior must lie downstream of the s-LNv molecular clock.

To test whether inducing Rho1 in s-LNvs alters their ability to signal, we measured the molecular clocks in DN1 clock neurons whose phase is set by the s-LNvs (Stoleru et al., 2005; Yao and Shafer, 2014; Yoshii et al., 2009). We found that the phase of the clock proteins VRI and PAR-Domain Protein 1 (PDP1) in DN1 clocks is shifted by ~6 hr between control and Rho1-induced flies after 3 days in DD (Figures 4B and S3B). Rhythmic DN1 clocks differ from their arrhythmicity in *Pdf^0* mutants (Yoshii et al., 2009). Thus, keeping s-LNv projections in a retracted state

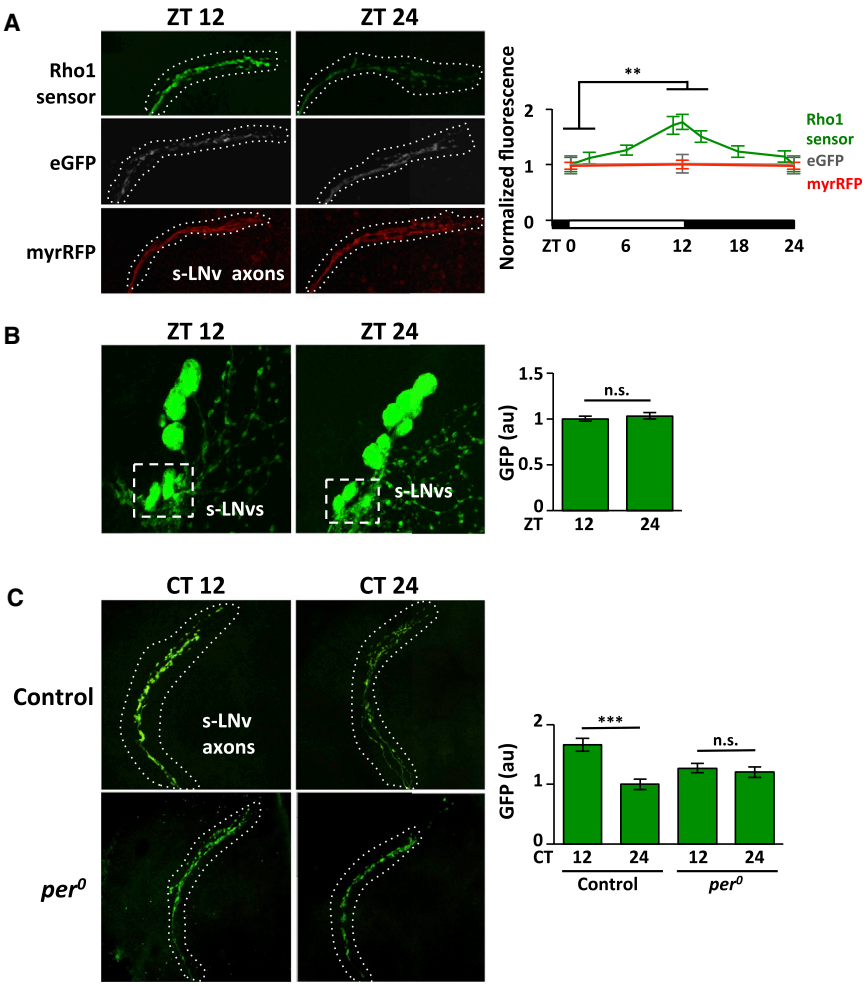

Figure 3. Circadian Oscillations in Rho1 Activity in s-LNv Axons

(A) Confocal images of s-LNv axons from flies expressing Rho1-activity sensor (*Pdf>PKNG58AeGFP*, green), eGFP (*Pdf>eGFP*, gray), or myrRFP (*Pdf>myrRFP*, red) stained with anti-GFP or anti-RFP. Graph shows average fluorescence levels in LD measured with Fiji with ZT0 data replotted at ZT24.

(B) Confocal images of s-LNv cell bodies from flies expressing Rho1-activity sensor with average GFP levels plotted on the right.

(C) Confocal images of s-LNv axons and termini from control (*Pdf>PKNG58AeGFP*) and per^0 flies (per^0; *Pdf > PKNG58AeGFP*) with average GFP levels plotted on the right.

Error bars show SEM. Statistical comparisons are with Student's t test. **p < 0.01, ***p < 0.001; n.s., non-significant.

seems to change rather than abolish s-LNv signaling, as is presumably the case in Pdf^0 mutants.

To test this idea, we built on the work of Stoleru et al. (2005). They had found that overexpressing the clock kinase Shaggy (Sgg)/GSK3 only in LNvs speeds up the molecular clock in many other clock neurons, leading to short period behavioral rhythms and indicating that s-LNvs determine the period of the entire clock network in DD. We reasoned that if retracting s-LNv projections alters their signaling, this should alter the period length of flies overexpressing *sgg*.

We measured the period of flies co-expressing *sgg* and either Rho1 or a control myrRFP transgene, again using *Pdf-Gal4, tubulin-Gal80^{ts}* to restrict expression to adults. Figure 4C shows that rhythmic flies expressing *sgg* and *myrRFP* have a short period of 21.4 hr, similar to expressing *sgg* throughout development. More *sgg*-expressing flies were arrhythmic at 30°C than at 25°C, probably due to higher Gal4 and/or Sgg activity at 30°C. In contrast, flies co-expressing *sgg* and Rho1 have a 23.1-hr period (Figure 4C; Table S1). Thus, we conclude that constitutively retracting s-LNv projections reduces their signaling strength and their ability to set the pace of the clock network.

LNv Structural Plasticity Is Important for Seasonal Adaptation

The circadian system is plastic with different neuronal groups taking the role of main oscillators as day length changes with the seasons (Stoleru et al., 2007; Zhang et al., 2010). s-LNvs are the dominant oscillators on short winter days, while the LNds, fifth s-LNv, and some DN1s assume control on long summer days (Stoleru et al., 2007). However, it is unclear how different oscillators take control of the network. Since retracting s-LNv projections reduces their ability to control the network (Figures 4B and 4C), we tested whether s-LNv plasticity is important for seasonal adaptation.

Flies were raised at 19°C and then transferred to 30°C and either winter (10:14) or summer (14:10) LD cycles. We compared the behavior of control flies (*Pdf, tub-Gal80^{ts} > myrGFP*) and experimental flies with induced expression of either Rho1 or $Rho1^{DN}$. Figure 4D shows that control flies shift their morning and evening activity peaks to align with seasonal dawn and dusk. However, flies with Rho1 induced in LNvs are active earlier before dawn in winter conditions than control flies, although their activity during summer is the same as control flies. Conversely, $Rho1^{DN}$ flies increase their activity later than control flies on summer mornings but behave like controls in winter (Figure 4D), and this is independent of activity levels (Figure S3C). We interpret these phenotypes as follows: high Rho1 activity constitutively retracts s-LNv projections, preventing s-LNvs from controlling the network in winter. In contrast, when s-LNvs cannot fully retract in $Rho1^{DN}$-induced flies, s-LNvs cannot cede control of the network in summer.

We also measured the behavior of Pdf^0 mutants in our winter and summer conditions. Pdf^0 flies show defective morning behavior in both conditions (Figure S3D) as in Renn

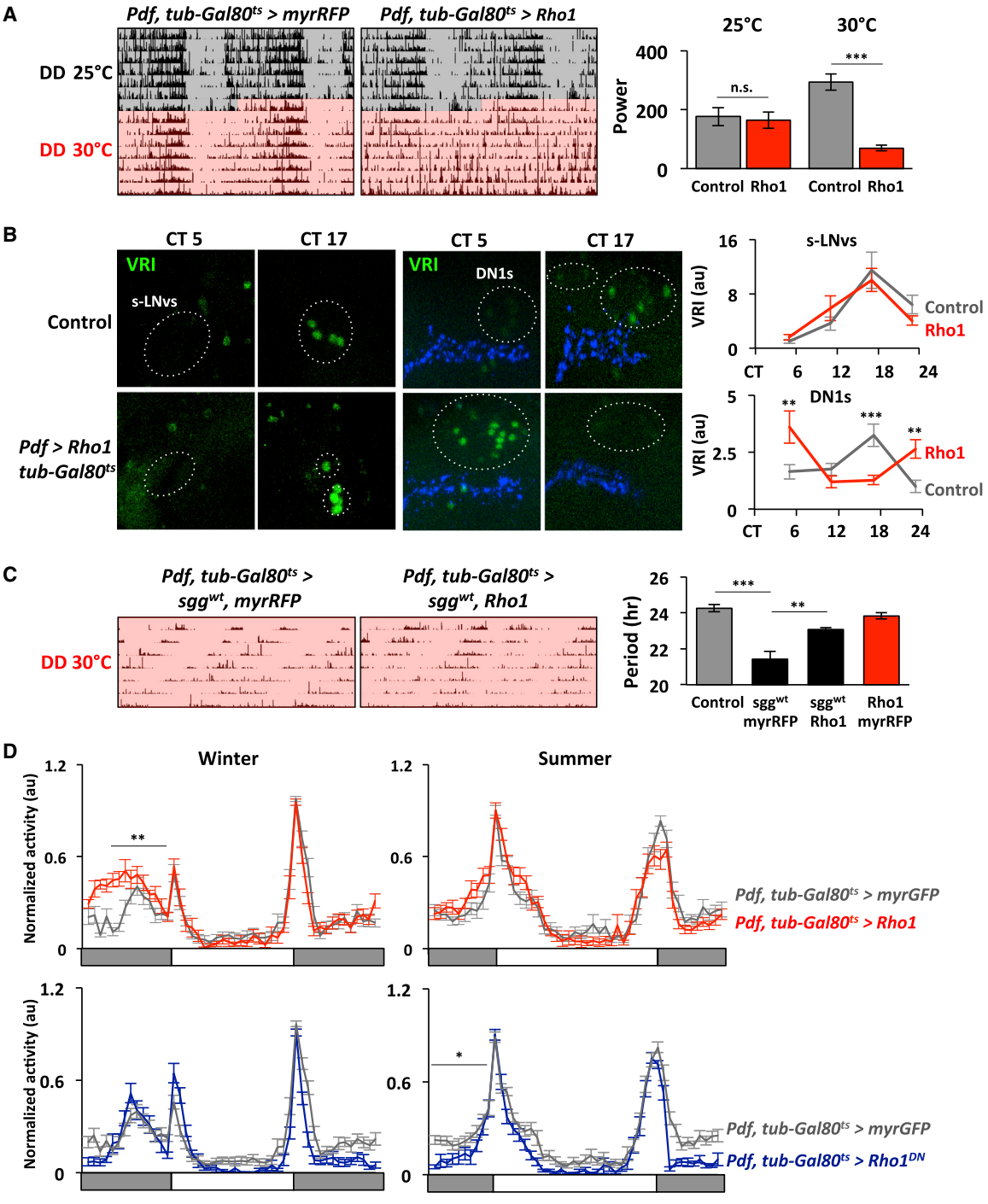

Figure 4. Rho1 Regulates an Output Pathway Important for Circadian Behavior and Seasonal Adaptation

(A) Left: actograms show locomotor activity in DD of control (*Pdf, tub-Gal80^{ts} > myrRFP*) and Rho1-inducible flies (*Pdf, tub-Gal80^{ts} > Rho1*) for 7 days at 25°C (gray) or 30°C (pink). Right: average rhythm power at 25°C and at 30°C in DD (also see Table S1).

(B) Flies were entrained to LD cycles at 19°C and then transferred to DD at 30°C. Confocal images of s-LNv cell bodies (left panels) and DN1 clock neurons (right panels) from control (*Pdf, tub-Gal80^{ts} > +*) and Rho1-induced flies (*Pdf, tub-Gal80^{ts} > Rho1*) stained with antibodies to VRI (green) and PDF (blue) at CT5 and CT17 on day 3 in DD. Graphs show average VRI fluorescence. The phase of the oscillation in DN1s was significantly different between genotypes ($p < 0.01$, ANOVA).

(C) Left: actograms of *Pdf, tub-Gal80^{ts} > sgg^{wt},myrRFP* and *Pdf, tub-Gal80^{ts} > sgg^{wt},Rho1* flies at 30°C in DD. Right: graph shows average period of rhythmic flies (also see Table S1).

(legend continued on next page)

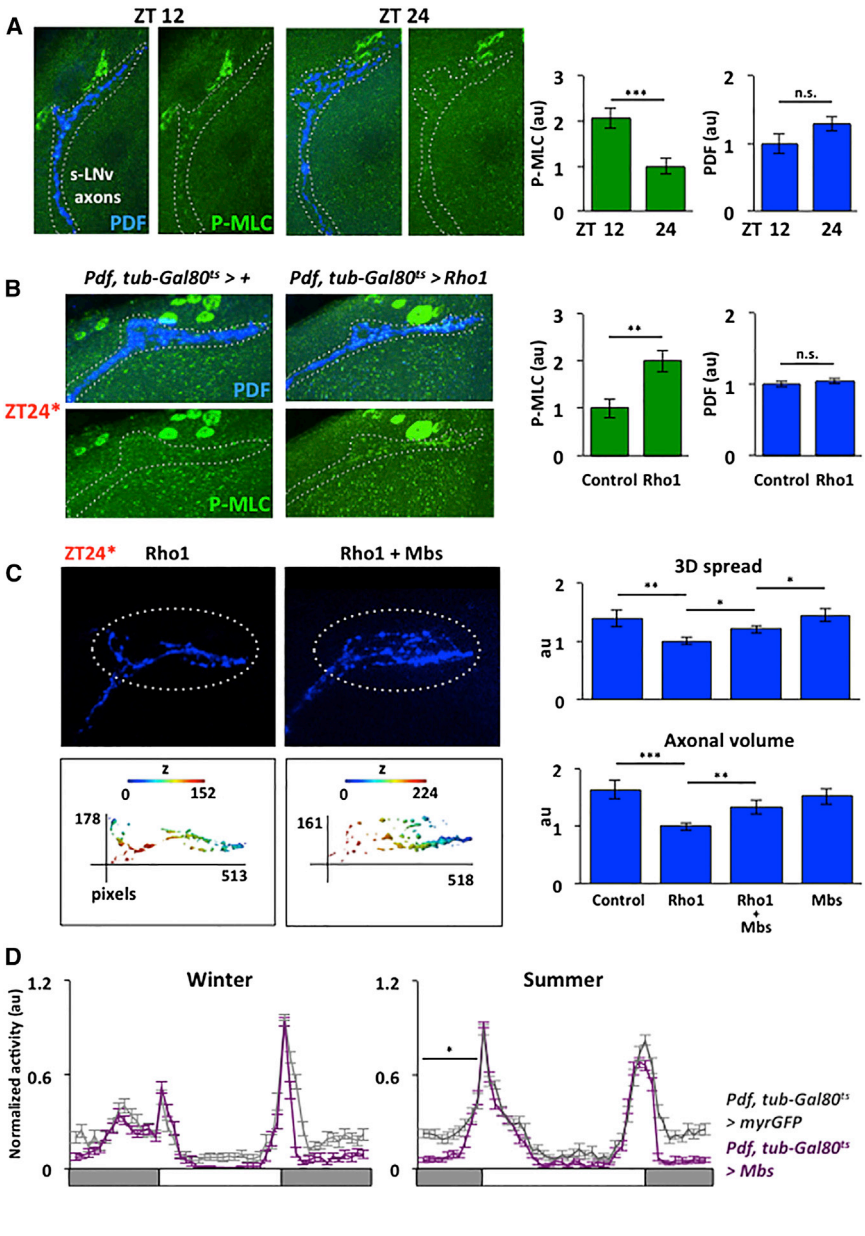

Figure 5. Rho1 Controls Rhythmic Myosin Light-Chain Phosphorylation in s-LNv Axons

(A) Confocal images of s-LNv axons at ZT12 and ZT24 stained with antibodies against P-MLC (green) and PDF (blue). Fluorescent intensity was measured with Fiji, and the normalized average is plotted on the right.

(B) Confocal images of s-LNv axons at ZT24* from *Pdf, tub-Gal80^{ts}* > + and *Pdf, tub-Gal80^{ts}* > *Rho1* flies stained and analyzed as in (A).

(C) Confocal images of s-LNv projections stained with anti-PDF (blue) and their 3D reconstructions as in Figure 1 from flies with Rho1-induced (Rho1) or both Rho1 and Mbs-induced (Rho1 + Mbs). Graphs show average 3D spread and axonal volume for control (*Pdf, tub-Gal80^{ts}* > *myrRFP* + *myrGFP*), Rho1 (*Pdf, tub-Gal80^{ts}* > *Rho1* + *myrRFP*), Rho1 + Mbs (*Pdf, tub-Gal80^{ts}* > *Rho1* + *Mbs*), and Mbs (*Pdf, tub-Gal80^{ts}* > *Mbs* + *myrRFP*) induced flies. 1 pixel = 0.12 μm and z-step is 1 μm.

(D) Locomotor activity of control (*Pdf, tub-Gal80^{ts}* > *myrGFP*, gray) and Mbs-induced (*Pdf, tub-Gal80^{ts}* > *Mbs*, purple) flies as in Figure 4D.

Error bars show SEM. Statistical comparisons are with Student's t test (A–C) and ANOVA (D). *p < 0.05, **p < 0.01, ***p < 0.001; n.s., non-significant. (See also Figure S4 and Table S1.)

et al. (1999) and Yoshii et al. (2009). Since the behavior of *Pdf* mutants differs from flies expressing Rho1 transgenes, this supports the idea that s-LNvs with altered plasticity still release PDF. Thus, structural plasticity likely modulates s-LNv signaling strength, with retracted s-LNv projections reducing signaling from s-LNvs to downstream cells. Reduced s-LNv signaling with Rho1 induced in LNvs probably explains why DN1 molecular clock oscillations do not stop as in *Pdf* mutants (Yoshii et al., 2009) but persist, albeit with altered phase (Figure 4B).

Rho1 Retracts s-LNvs via Myosin Phosphorylation

Billuart et al. (2001) showed that Rho1 retracts axonal branches during *Drosophila* mushroom body development by phosphorylating myosin light chain (MLC) to contract actin filaments. To understand how Rho1 regulates s-LNv plasticity, we asked whether phosphorylated MLC (P-MLC) levels change between dusk and dawn in s-LNv axons using a P-MLC specific antibody (Lee and Treisman, 2004). We found that P-MLC levels in s-LNv axons were 2-fold higher at ZT12 than ZT24 (Figure 5A). These data are consistent with higher Rho1 activity at dusk and serve as an independent marker of endogenous Rho1 activity rhythms. P-MLC oscillations were blocked in *per^{0}* flies (Figure S4A), indicating that MLC phosphorylation is clock controlled in s-LNv axons, like Rho1 activity. To test whether Rho1 is responsible for MLC phosphorylation, we induced Rho1 for 12 hr. This increased P-MLC levels at ZT24* ~2-fold over controls (Figure 5B). Thus, we conclude that high Rho1 activity in s-LNv axons around dusk increases MLC phosphorylation.

(D) Locomotor activity of control (*Pdf, tub-Gal80^{ts}* > *myrGFP*, gray), Rho1- (*Pdf, tub-Gal80^{ts}* > *Rho1*, red) and Rho1^{DN}-induced flies (*Pdf, tub-Gal80^{ts}* > *Rho1^{DN}*, blue) in winter (10L:14D) or summer (14L:10D) light conditions.

Error bars show SEM. Statistical comparisons are with Student's t test (A–C) and ANOVA (D). *p < 0.05, **p < 0.01, ***p < 0.001; n.s., non-significant. (See also Figure S3.)

Rho1 regulates MLC phosphorylation through ROCK (Rho-associated protein kinase) and Mbs (Myosin binding subunit, (Kimura et al., 1996). When Rho1 binds ROCK and Mbs, ROCK phosphorylates and inhibits Mbs, an MLC Phosphatase (MLCP) subunit (Hartshorne et al., 1998). Phosphorylated Mbs decreases MLCP activity, which increases MLC phosphorylation and actomyosin contraction (Kawano et al., 1999; Kimura et al., 1996). If the myosin pathway is downstream of Rho1 in s-LNvs, we hypothesized that overexpressing *Mbs* would rescue Rho1-induced retraction. We found that the axonal volume and 3D spread of s-LNv projections at ZT24* were higher when *Mbs* was co-induced with *Rho1* than with *Rho1* alone (Figure 5C). Similarly, the behavioral arrhythmicity of flies overexpressing *Rho1* from birth was rescued by overexpressing *Mbs* (Figure S4B; Table S1).

Next, we tested whether MLC phosphorylation is required for s-LNv projections to retract at dusk. We induced Mbs to trigger MLC dephosphorylation for 12 hr starting either at dawn or dusk and assayed s-LNv morphology. We found that s-LNv projections in Mbs-induced flies had significantly higher 3D spread and axonal volume at ZT12* than control flies (Figure S4C). This suggests that MLC phosphorylation is required for retraction and that Mbs activity is normally rhythmic and low at dusk when Rho1 activity is high.

We also tested how Mbs induction affects seasonal adaptation. We found that Mbs-induced flies adapt normally to winter light conditions but less well to summer (Figure 5D), like $Rho1^{DN}$ (Figure 4D). Given that s-LNv projections can never fully retract after inducing Mbs or $Rho1^{DN}$ (Figures 2 and S4C), these results strengthen the argument that seasonal adaptation requires structural plasticity. We propose that Rho1 promotes retraction of s-LNv projections at dusk by opposing Mbs activity and promoting MLC phosphorylation.

Pura Is a Clock-Regulated Rho1 GEF that Regulates Rhythmic Rho1 Activity in s-LNvs

Clock-regulated Rho1 activity in s-LNv axons could be explained by rhythms in a Rho1 GEF peaking at dusk and/or a Rho1 GAP peaking at dawn. Our expression profiles of larval LNvs revealed that *CG33275*, a previously uncharacterized and predicted Rho GEF, is clock-regulated and rhythmically expressed in LD and DD, with RNA levels peaking around dusk (Mizrak et al., 2012; Ruben et al., 2012). *CG33275* is also rhythmically expressed in adult s-LNvs, with higher expression at ZT12 than ZT24 (Kula-Eversole et al., 2010). Phylogenetic tree analysis (using http://www.ensembl.org/index.html) and reciprocal BLAST showed that *CG33275* is orthologous to human Puratrophin-1 (Purkinje cell atrophy associated protein-1/*Plekhg4*), which functions as a Rho family GEF in vitro (Gupta et al., 2013; Ishikawa et al., 2005). Puratrophin-1 is also rhythmically expressed in the mouse pituitary (Pizarro et al., 2013), suggesting that it has a circadian function. Thus, we named *CG33275 Puratrophin-1-like* (*Pura*). Pura is 56% identical and 72% homologous to human Puratrophin-1 over the adjoining Dibble-homology and Pleckstrin-like homology domains that are a signature of GEFs for Rho family GTPases (Schmidt and Hall, 2002).

To test whether rhythmic *Pura* expression results from transcriptional regulation, we used a *Pura-Gal4* line inserted 45 bp upstream of the predicted start site of the *Pura-B* transcript. We crossed *Pura-Gal4* flies to a nuclear-localized *UAS-destabilized-GFP* transgene and found that GFP levels in s-LNvs were higher at ZT14 than ZT2 (Figure S5A), in phase with *Pura* RNA. This rhythm is specific to *Pura-Gal4* since *Pdf-Gal4* showed no GFP rhythms (Figure S5A). *Pura* may be a direct CLK/CYC target since there are two E-boxes in the first 1.5 kb upstream of *Pura-Gal4*.

We used genetic interactions to test whether Pura can act as a Rho1 GEF in LNvs. We first confirmed that *UAS-Pura*^{RNAi} and *UAS-Pura*^{shRNA} transgenes that target different *Pura* sequences reduce *Pura* RNA levels (Figure S5B). We found that the behavioral arrhythmicity of flies overexpressing *Rho1* from birth was rescued by co-expressing either *Pura*^{RNAi} or *Pura*^{shRNA} (Figure S5C; Table S1). This effect is specific for Rho1. First, we found that the arrhythmic phenotype of flies expressing a constitutively active Rho1 ($Rho1^{CA}$) in LNvs was unaltered by co-expressing *Pura*^{RNAi} (Figure S5C; Table S1). Since $Rho1^{CA}$ binds GTP independently of GEFs, we conclude that Pura only regulates Rho1 activity when Rho1 is GEF dependent. Second, we found that *Rac1* overexpression in LNvs lengthens period to 25 hr and that this was unaltered by *Pura*^{RNAi} (Table S1). Thus, Pura acts on Rho1 but not Rac1.

To test whether Pura is the Rho1 GEF responsible for circadian Rho1 activity in s-LNv axons, we used the Rho1 sensor to measure Rho1 activity. The data in Figure 6A show that *Pura*^{RNAi} and *Pura*^{shRNA} block rhythmic Rho1 activity and reduce Rho1 activity at CT12 to levels comparable to control s-LNv axons at CT24. Reducing endogenous *Pura* levels did not alter Rho1 activity in s-LNv cell bodies (data not shown), indicating that Pura only regulates Rho1 activity in axons. Taken together, we conclude that Pura regulates the timing and localization of Rho1 activity that connects the core clock to s-LNv outputs.

Pura Is Required for s-LNv Structural Plasticity and Seasonal Adaptation

We also tested whether normal *Pura* levels are required for s-LNv structural plasticity. We induced *Pura*^{RNAi} starting at dusk or dawn and assayed s-LNv projections 12 hr later. We found that *Pura*^{RNAi} expression significantly increased the 3D spread and axonal volume at ZT12* compared to control flies (Figure 6B). Thus, maximal *Pura* expression is required for full retraction at dusk. In contrast, s-LNv projections in *Pura*^{RNAi} flies were similar to control flies at ZT24*. *Pura*'s time-specific effect on Rho1 activity and LNv projections is consistent with the timing of both *Pura* RNA and Rho1 activity rhythms.

We also tested whether reducing *Pura* expression can override Rho1-induced retractions in s-LNv projections. We induced wild-type Rho1 for 12 hr as in Figure 1B either with or without *Pura*^{RNAi}. Figure 6C shows that inducing *Pura*^{RNAi} along with *Rho1* (*Pdf, tub-Gal80*^{ts} > *Rho1* + *Pura*^{RNAi}) restored the axonal volume and 3D spread of s-LNv projections to control ZT24* levels. In addition, inducing *Pura*^{RNAi} also prevented overexpressed *Rho1* from increasing MLC phosphorylation at ZT24* (Figure S5D). Thus, we conclude that Rho1 requires sufficient *Pura* expression to retract s-LNv axons via actin-related structural changes and that rhythmic *Pura* expression normally limits the timing of Rho1 activity.

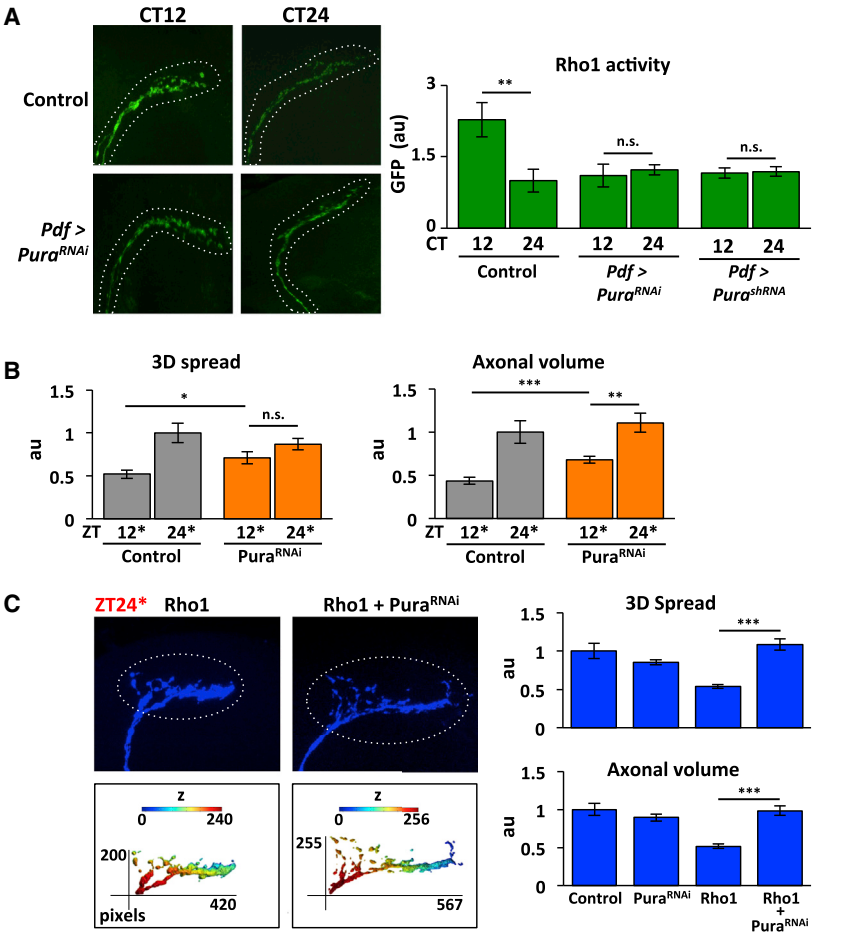

Figure 6. *Pura* Is a Clock-Regulated Rho1 GEF that Activates Rho1 in s-LNv Axons at Dusk and Is Required for Seasonal Adaptation

(A) Confocal images of s-LNv axons at CT12 and CT24 on day 1 in DD from control (*Pdf* > *PKNG58AeGFP* + *corazonin*^{RNAi}) and *Pdf* > *Pura*^{RNAi} flies (*Pdf* > *PKNG58AeGFP* + *Pura*^{RNAi}) expressing the Rho1-activity sensor (green) as in Figure 3. Graph shows the average fluorescence intensity of the Rho1-sensor in s-LNv axons from the above genotypes and from *Pdf* > *Pura*^{shRNA} flies (*Pdf* > *PKNG58AeGFP* + *Pura*^{shRNA}).

(B) s-LNv projections were stained with anti-PDF and quantified as in Figure 1 from control (*Pdf, tub-Gal80*^{ts} > *myrRFP*) and *Pura*^{RNAi} flies (*Pdf, tub-Gal80*^{ts} > *Pura*^{RNAi}) and entrained and shifted to 30°C for 12 hr as in Figure 2.

(C) Confocal images of s-LNv projections stained with PDF (blue) and their 3D reconstructions from flies with either *Rho1* (*Pdf, tub-Gal80*^{ts} > *Rho1* + *myrRFP*) or *Rho1* and *Pura*^{RNAi} (*Pdf, tub-Gal80*^{ts} > *Rho1* + *Pura*^{RNAi}) induced for 12 hr and fixed at ZT24*. Graphs show the average 3D spread and axonal volume. 1 pixel = 0.12 μm and z-step is 1 μm. Error bars show SEM.

(D) Locomotor activity of control (*Pdf, tub-Gal80*^{ts} > *myrGFP*, gray) and *Pura*^{shRNA}-induced flies (*Pdf, tub-Gal80*^{ts} > *Pura*^{shRNA}, orange) as in Figure 4D.

Error bars show SEM. Statistical comparisons are with Student's t test (A–C) and ANOVA (D). *p < 0.05, **p < 0.01, ***p < 0.001; n.s., non-significant. (See also Figure S5 and Table S1.)

We also tested *Pura*'s importance in seasonal adaptation. We found that inducing *Pura*^{shRNA} reduced morning adaptation in summer conditions but did not affect winter behavior (Figure 6D), just like Rho1^{DN} and Mbs flies (Figures 4D and 5D).

Flies overexpressing *Pura*^{RNAi}, *Pura*^{shRNA}, *Mbs*, or *Rho1*^{DN} have normal locomotor activity in DD, in contrast to Rho1 induction, which promotes arrhythmicity (Table S1). We propose that Rho1 activity is normally limited in DD and winter since s-LNvs need to dominate the clock network and thus be in an expanded or permissive state for communication (Stoleru et al., 2005). However, when s-LNvs cede control of the network to other clock neurons during summer (Stoleru et al., 2007), Rho1 activity needs to be maximal, to maintain s-LNv projections in a retracted state that reduces signaling.

Although *Pdf, tub-Gal80*^{ts} > *Pura*^{shRNA} flies are rhythmic in DD (Table S1), we tested their molecular clock after 3 days at 30°C. We found that VRI oscillations were similar to control flies in s-LNvs and DN1s (Figure S5E; data not shown) but had slightly altered rhythms in LNds (Figure S5E), whose connectivity with s-LNvs is rhythmic (Gorostiza et al., 2014). Thus, s-LNv plasticity is required for optimal signaling with downstream neurons.

s-LNv Plasticity Changes Clock Network Communication

Gorostiza et al. (2014) recently showed that rhythms in s-LNv projection morphology are accompanied by rhythms in the number of pre-synaptic active zones. We used a fluorescently tagged Bruchpilot-short (BRP$^{short-strawberry}$) transgene to detect active zones and confirmed that s-LNv projections have more BRP puncta at ZT2* than ZT14* (Figure 7A and S6). We then tested the role of Rho1 and Pura in this rhythm. The data in Figure 7A show that inducing Rho1 for 14 hr reduces the number of active zones at ZT2* to control levels at ZT14* but does not change the low levels at ZT14*. The complementary experiment with

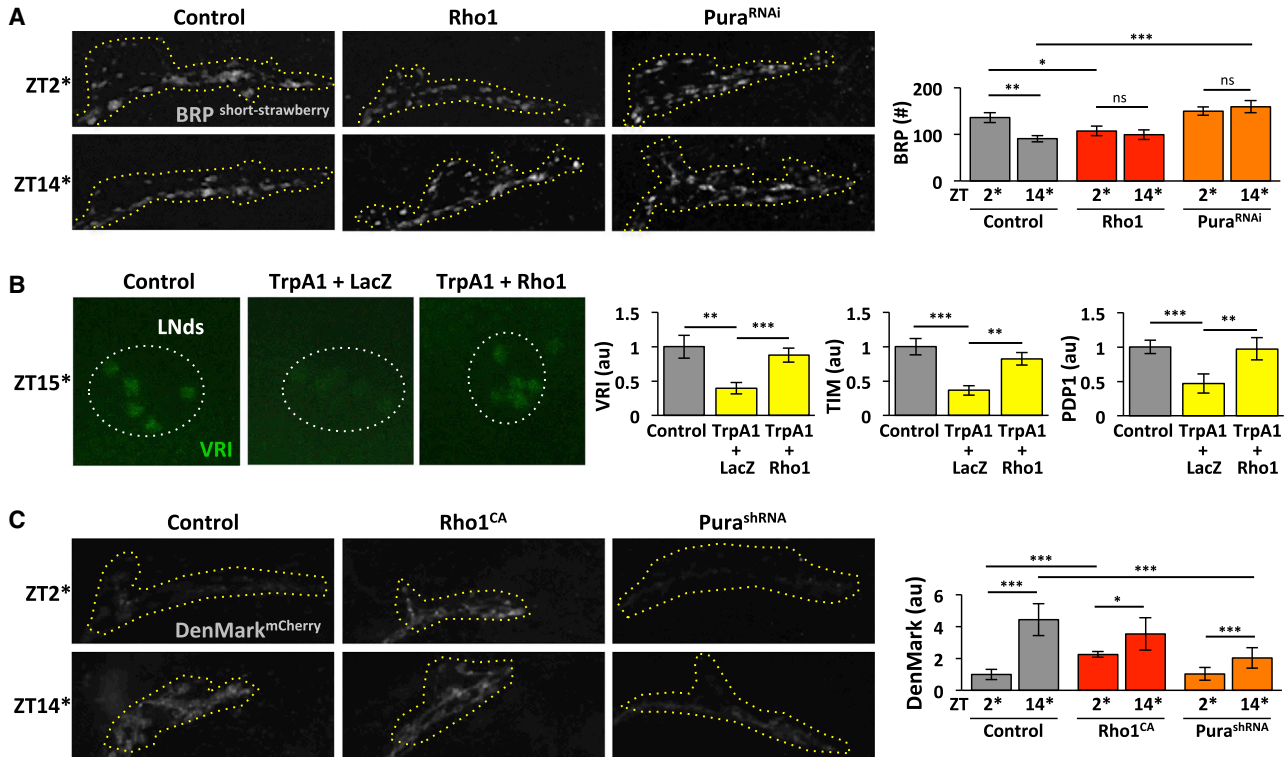

Figure 7. Pura and Rho1 Regulate Synaptic Plasticity

(A) Confocal images of s-LNv projections at ZT2* and ZT14* from control (Pdf, tub-Gal80^{ts} > brp$^{short\text{-}strawberry}$ + LacZ), Rho1 (Pdf, tub-Gal80^{ts} > brp$^{short\text{-}strawberry}$ + Rho1), and Pura^{RNAi} (Pdf, tub-Gal80^{ts} > brp$^{short\text{-}strawberry}$ + Pura^{RNAi}) flies. Flies were raised at 19°C and entrained in LD cycles at 19°C for at least 3 days before shifting to 30°C, starting at ZT12 or ZT24. Flies were dissected 14 hr later at ZT2* and ZT14*, respectively, and brains stained with αDsRed (gray) to visualize Brp. Graph shows average numbers of active zones.

(B) Confocal images of LNd clock neurons from control (Pdf, tub-Gal80^{ts} > myrRFP), TrpA1 + LacZ (Pdf, tub-Gal80^{ts} > TrpA1, LacZ), and TrpA1 + Rho1 (Pdf, tub-Gal80^{ts} > TrpA1, Rho1) flies. Flies were raised and entrained in LD at 19°C before shifting to 30°C for 3 hr at ZT12 and dissecting 3 hr later at ZT15*. Brains were stained for VRI (green), TIM, and PDP1. Quantification was as in Figure 4B.

(C) Confocal images of s-LNv projections at ZT2* (top) and ZT14* (bottom) from control (Pdf, tub-Gal80^{ts} > DenMark + LacZ), Rho1 (Pdf, tub-Gal80^{ts} > DenMark + Rho1^{CA}) and Pura^{shRNA} (Pdf, tub-Gal80^{ts} > DenMark + Pura^{shRNA}) flies. Flies were handled as in (A), and brains were stained with αDsRed (gray). Quantification of average DenMark fluorescence levels was performed with Fiji.

Error bars show SEM. Statistical comparisons are with Student's t test. *p < 0.05, **p < 0.01, ***p < 0.001; n.s., non-significant. (See also Figure S6.)

Pura^{RNAi} gave the opposite results: active zone numbers were now constitutively high.

Changes in the number of active zones support the idea that s-LNv plasticity changes signaling. To test this idea further and to test how rapidly Rho1 can regulate s-LNv signaling, we built on the finding that s-LNv firing rapidly reduces levels of the core clock protein TIM in LNd clock neurons (Guo et al., 2014). We induced expression and activity of TrpA1 in s-LNvs for 3 hr starting at ZT12 and measured levels of VRI, TIM, and PDP1 in LNds at ZT15*. Inducing LNv firing reduced levels of all three proteins (Figure 7B). However, co-inducing Rho1 along with TrpA1 in LNvs blocked these rapid effects of LNvs on the LNd molecular clock (Figure 7B). Thus, Rho1 activity can modulate the effect of LNv firing on downstream neurons.

Inputs from other clock neurons help synchronize individual s-LNv molecular clocks and regulate their neuronal activity (Collins et al., 2012, 2014). Since electron microscopy (EM) studies of s-LNv axonal projections had revealed they have input synapses (Yasuyama and Meinertzhagen, 2010), we tested whether s-LNv plasticity is also associated with altered accumulation of post-synaptic components. We used DenMark to mark dendrites (Nicolaï et al., 2010) and found that DenMark levels at ZT14* are ~4-fold higher than at ZT2* (Figure 7C). Increasing Rho1 activity by inducing Rho1^{CA} increased the normally low DenMark levels at ZT2*, whereas reducing *Pura* levels using *Pura^{shRNA}* reduced the high DenMark levels at ZT14*, although both manipulations left reduced amplitude DenMark oscillations. The antiphase rhythms of DenMark and BRP in wild-type s-LNvs suggest that s-LNv morphological plasticity is accompanied by a switch from predominantly receiving signals around dusk to predominantly sending signals around dawn. This synaptic plasticity is also regulated by Pura and Rho1.

DISCUSSION

Directly linking plasticity to behavior is challenging in the adult brain. We took advantage of predictable and quantifiable changes in s-LNv structure and the precision of *Drosophila*

genetics for spatial and temporal manipulation. We identified circadian rhythms in Rho1 GTPase activity in s-LNv axons that are regulated by rhythmic transcription of *Pura*, a Rho1 GEF. Pura activates Rho1 to retract s-LNv axons, decrease active zone numbers and reduce s-LNvs' influence on the clock network. Thus, we make strong links between transcription, plasticity, network hierarchy and behavior.

Mammalian SCN pacemaker neurons show rhythms in post-synaptic densities and neuron-glia connections (Becquet et al., 2008; Girardet et al., 2010). Even liver cells show daily rhythms in actin dynamics and cell size (Gerber et al., 2013). It will be interesting to test whether SCN synapses show Rho-regulated plasticity as a potentially conserved mechanism to regulate clock neuron communication.

SCA and Pura

Mutations in human *Puratrophin-1* are linked to Spinocerebellar ataxia (SCA), a neurodegenerative disease affecting cerebellar Purkinje cells (Ishikawa et al., 2005). Atrophic Purkinje cells from these SCA patients have cytoplasmic aggregates containing Puratrophin-1 and the actin-binding protein Spectrin (Ishikawa et al., 2005), consistent with fly and mammalian proteins both having actin-related functions.

The SCA-associated mutations reduce *Puratrophin-1* RNA levels (Amino et al., 2007; Ishikawa et al., 2005). Thus, cerebellar *Puratrophin-1* expression seems to be tightly regulated like *Pura* in s-LNvs. We speculate that low *Puratrophin-1* expression reduces activity of RhoA, the Rho1 ortholog. This could misregulate the ROCK/myosin pathway, reducing plasticity and neuronal connectivity and lead to Purkinje cell atrophy.

Rho GTPases and Neuronal Signaling

Rho GTPases are regulated by Rho GEFs and GAPs (Van Aelst and D'Souza-Schorey, 1997). Pura seems to provide spatiotemporal specificity for Rho1 in s-LNvs. Pura protein localization likely restricts Rho1 activity to axons and rhythmic *Pura* expression limits the timing of Rho1 activity.

Gorostiza et al. (2014) added two levels of s-LNv plasticity beyond morphology: s-LNvs change connections with other neurons over 24 hr and show rhythms in the numbers of pre-synaptic sites. We found rhythms in post-synaptic markers at s-LNv termini in antiphase to pre-synaptic markers. Since Rho1 activity regulates s-LNv structural and synaptic plasticity, Rho1 activity profoundly influences the effectiveness of s-LNv signaling and can modulate the intrinsic excitability of LNvs.

We propose that external cues can control Rho1 activity. Yuan et al. (2011) showed that long days reduce larval LNv dendrite length. We propose that long days keep adult s-LNv axons retracted by increasing Rho1 activity, while s-LNv firing around dawn decreases Rho1 activity to allow axonal expansion. We recently showed that increased LNv activity reduces *Pura* RNA levels (Mizrak et al., 2012). Thus, *Pura* expression may integrate clock state and electrical activity.

s-LNv plasticity may also involve Rho GTPases such as Rac1 and Cdc42 at dawn. It will be interesting to test whether s-LNv plasticity is regulated by the opposing dynamics of different Rho GTPases. These neurons regulating innate behavior are surprisingly plastic and their intrinsic transcriptional programs make s-LNvs an exciting system to understand the role of actin dynamics in structural and synaptic plasticity.

EXPERIMENTAL PROCEDURES

Adult Locomotor Activity

For locomotor activity experiments that included temperature induction, adult flies were entrained for 3 days in 12:12 LD cycles at 19°C and then transferred to DD at 25°C or 30°C. For other experiments, adults were entrained for 3 days in 12:12 LD cycles at 25°C before transfer to DD. Locomotor activity was recorded using the DAM system (TriKinetics) and we used χ^2 analysis in ClockLab (Actimetrics) to calculate the power above the significance line ($p < 0.01$) for each fly. Flies with a power <100 were considered arrhythmic and excluded from period calculations but included in average power calculations. Flies were kept for 5 days at 30°C in 10:14 and 14:10 LD cycles for winter and summer conditions respectively. Activity data from the last 2 days were averaged, normalized, and plotted using a bin size of 30 min. Morning anticipation was measured as the activity 5 hr before dawn (ZT19-ZT24).

Immunocytochemistry

Immunocytochemistry was carried out as in Collins et al. (2012, 2014). Antibodies are described in the Supplemental Information. Images were scanned on the 20× lens of a Leica SP5 confocal microscope with 4-6.1× digital zoom. For P-MLC staining, brains were cleared through an isopropanol series and mounted in Murray Clear (1:2 benzyl alcohol: benzyl benzoate) as in Veeman and Smith (2013). Mean staining intensity was quantified using Fiji (http://pacific.mpi-cbg.de/wiki/index.php/Main_Page), with background staining levels subtracted. BRP puncta were quantified as in Gorostiza et al. (2014).

Quantification of Structural Plasticity

127 × 127 μm confocal stack jpg images with 1024 × 1024 pixel resolution were imported into MATLAB and s-LNv projections starting from where axons turn dorsally were selected for quantification. The MATLAB script generates a 3D surface contour over regions (pixels) with >70% of the maximum fluorescent intensity to identify s-LNv projections. A 3D curve that runs through the pixels that form the s-LNv projections is then computed along with the average spread in x, y, and z axes (Figure S1A). We mutliply these values to obtain the 3D spread. The script also calculates the total amount of pixels, which is the axonal volume. See Supplemental Experimental Procedures for a detailed description.

SUPPLEMENTAL INFORMATION

Supplemental Information includes Supplemental Experimental Procedures, one table, and six figures and can be found with this article online at http://dx.doi.org/10.1016/j.cell.2015.07.010.

ACKNOWLEDGMENTS

We thank Vivian Budnik, Paul Hardin, Brian McCabe, Tim Mosca, Jae Park, Michael Rosbash, Amita Sehgal, Stephan Sigrist, Sergio Simões, Jessica Treisman, the DSHB and the VDRC, Kyoto and Bloomington Stock Centers for flies and antibodies. We thank Anita Burgos and Samantha Raymond for their contributions and Hsaio-Yun Liu for advice on shRNA. We thank Rich Bonneau, Lionel Christiaen, Claude Desplan, Erik Herzog, Adrian Rothenfluh, Chris Rushlow, and Mark Siegal for invaluable discussions, Claire Bertet, Matthieu Cavey, Ben Collins, Chris Hackley, and Zhonghua Zhu for comments on the manuscript, and Erin Meekhof for making the graphical abstract. We also thank Herman Wijnen for communicating unpublished data. This investigation was conducted in facilities constructed with support from Research Facilities Improvement Grant Number C06 RR-15518-01 from the NCRR, NIH. Imaging was performed at NYU's Center for Genomics & Systems Biology. A.P. was partly supported by NYU's GSAS MacCracken Program and a Dean's Dissertation Fellowship. T.P.S. was partly supported by an NYU Courant Institute postdoctoral fellowship. This work was supported by NIH grants GM063911 and NS077156 to J.B.

Received: June 5, 2014
Revised: March 19, 2015
Accepted: June 13, 2015
Published: July 30, 2015

REFERENCES

Amino, T., Ishikawa, K., Toru, S., Ishiguro, T., Sato, N., Tsunemi, T., Murata, M., Kobayashi, K., Inazawa, J., Toda, T., and Mizusawa, H. (2007). Redefining the disease locus of 16q22.1-linked autosomal dominant cerebellar ataxia. J. Hum. Genet. *52*, 643–649.

Becquet, D., Girardet, C., Guillaumond, F., François-Bellan, A.M., and Bosler, O. (2008). Ultrastructural plasticity in the rat suprachiasmatic nucleus. Possible involvement in clock entrainment. Glia *56*, 294–305.

Billuart, P., Winter, C.G., Maresh, A., Zhao, X., and Luo, L. (2001). Regulating axon branch stability: the role of p190 RhoGAP in repressing a retraction signaling pathway. Cell *107*, 195–207.

Cao, G., and Nitabach, M.N. (2008). Circadian control of membrane excitability in *Drosophila melanogaster* lateral ventral clock neurons. J. Neurosci. *28*, 6493–6501.

Cao, G., Platisa, J., Pieribone, V.A., Raccuglia, D., Kunst, M., and Nitabach, M.N. (2013). Genetically targeted optical electrophysiology in intact neural circuits. Cell *154*, 904–913.

Collins, B., Kane, E.A., Reeves, D.C., Akabas, M.H., and Blau, J. (2012). Balance of activity between LNvs and glutamatergic dorsal clock neurons promotes robust circadian rhythms in *Drosophila*. Neuron *74*, 706–718.

Collins, B., Kaplan, H.S., Cavey, M., Lelito, K.R., Bahle, A.H., Zhu, Z., Macara, A.M., Roman, G., Shafer, O.T., and Blau, J. (2014). Differentially timed extracellular signals synchronize pacemaker neuron clocks. PLoS Biol. *12*, e1001959.

Fernández, M.P., Berni, J., and Ceriani, M.F. (2008). Circadian remodeling of neuronal circuits involved in rhythmic behavior. PLoS Biol. *6*, e69.

Gerber, A., Esnault, C., Aubert, G., Treisman, R., Pralong, F., and Schibler, U. (2013). Blood-borne circadian signal stimulates daily oscillations in actin dynamics and SRF activity. Cell *152*, 492–503.

Girardet, C., Blanchard, M.P., Ferracci, G., Lévêque, C., Moreno, M., François-Bellan, A.M., Becquet, D., and Bosler, O. (2010). Daily changes in synaptic innervation of VIP neurons in the rat suprachiasmatic nucleus: contribution of glutamatergic afferents. Eur. J. Neurosci. *31*, 359–370.

Gonzalez-Billault, C., Muñoz-Llancao, P., Henriquez, D.R., Wojnacki, J., Conde, C., and Caceres, A. (2012). The role of small GTPases in neuronal morphogenesis and polarity. Cytoskeleton (Hoboken) *69*, 464–485.

Gorostiza, E.A., Depetris-Chauvin, A., Frenkel, L., Pírez, N., and Ceriani, M.F. (2014). Circadian pacemaker neurons change synaptic contacts across the day. Curr. Biol. *24*, 2161–2167.

Guo, F., Cerullo, I., Chen, X., and Rosbash, M. (2014). PDF neuron firing phase-shifts key circadian activity neurons in *Drosophila*. eLife *3*, e02780.

Gupta, M., Kamynina, E., Morley, S., Chung, S., Muakkassa, N., Wang, H., Brathwaite, S., Sharma, G., and Manor, D. (2013). Plekhg4 is a novel Dbl family guanine nucleotide exchange factor protein for Rho family GTPases. J. Biol. Chem. *288*, 14522–14530.

Hall, A. (2012). Rho family GTPases. Biochem. Soc. Trans. *40*, 1378–1382.

Hartshorne, D.J., Ito, M., and Erdödi, F. (1998). Myosin light chain phosphatase: subunit composition, interactions and regulation. J. Muscle Res. Cell Motil. *19*, 325–341.

Ishikawa, K., Toru, S., Tsunemi, T., Li, M., Kobayashi, K., Yokota, T., Amino, T., Owada, K., Fujigasaki, H., Sakamoto, M., et al. (2005). An autosomal dominant cerebellar ataxia linked to chromosome 16q22.1 is associated with a single-nucleotide substitution in the 5′ untranslated region of the gene encoding a protein with spectrin repeat and Rho guanine-nucleotide exchange-factor domains. Am. J. Hum. Genet. *77*, 280–296.

Kawano, Y., Fukata, Y., Oshiro, N., Amano, M., Nakamura, T., Ito, M., Matsumura, F., Inagaki, M., and Kaibuchi, K. (1999). Phosphorylation of myosin-binding subunit (MBS) of myosin phosphatase by Rho-kinase in vivo. J. Cell Biol. *147*, 1023–1038.

Kimura, K., Ito, M., Amano, M., Chihara, K., Fukata, Y., Nakafuku, M., Yamamori, B., Feng, J., Nakano, T., Okawa, K., et al. (1996). Regulation of myosin phosphatase by Rho and Rho-associated kinase (Rho-kinase). Science *273*, 245–248.

Kula-Eversole, E., Nagoshi, E., Shang, Y., Rodriguez, J., Allada, R., and Rosbash, M. (2010). Surprising gene expression patterns within and between PDF-containing circadian neurons in *Drosophila*. Proc. Natl. Acad. Sci. USA *107*, 13497–13502.

Lee, A., and Treisman, J.E. (2004). Excessive Myosin activity in *mbs* mutants causes photoreceptor movement out of the *Drosophila* eye disc epithelium. Mol. Biol. Cell *15*, 3285–3295.

Matsuzaki, M., Honkura, N., Ellis-Davies, G.C., and Kasai, H. (2004). Structural basis of long-term potentiation in single dendritic spines. Nature *429*, 761–766.

May, A. (2011). Experience-dependent structural plasticity in the adult human brain. Trends Cogn. Sci. *15*, 475–482.

McGuire, S.E., Le, P.T., Osborn, A.J., Matsumoto, K., and Davis, R.L. (2003). Spatiotemporal rescue of memory dysfunction in *Drosophila*. Science *302*, 1765–1768.

Meredith, A.L., Wiler, S.W., Miller, B.H., Takahashi, J.S., Fodor, A.A., Ruby, N.F., and Aldrich, R.W. (2006). BK calcium-activated potassium channels regulate circadian behavioral rhythms and pacemaker output. Nat. Neurosci. *9*, 1041–1049.

Mizrak, D., Ruben, M., Myers, G.N., Rhrissorrakrai, K., Gunsalus, K.C., and Blau, J. (2012). Electrical activity can impose time of day on the circadian transcriptome of pacemaker neurons. Curr. Biol. *22*, 1871–1880.

Nicolaï, L.J., Ramaekers, A., Raemaekers, T., Drozdzecki, A., Mauss, A.S., Yan, J., Landgraf, M., Annaert, W., and Hassan, B.A. (2010). Genetically encoded dendritic marker sheds light on neuronal connectivity in *Drosophila*. Proc. Natl. Acad. Sci. USA *107*, 20553–20558.

Park, J.H., Helfrich-Förster, C., Lee, G., Liu, L., Rosbash, M., and Hall, J.C. (2000). Differential regulation of circadian pacemaker output by separate clock genes in *Drosophila*. Proc. Natl. Acad. Sci. USA *97*, 3608–3613.

Pizarro, A., Hayer, K., Lahens, N.F., and Hogenesch, J.B. (2013). CircaDB: a database of mammalian circadian gene expression profiles. Nucleic Acids Res. *41*, D1009–D1013.

Renn, S.C., Park, J.H., Rosbash, M., Hall, J.C., and Taghert, P.H. (1999). A *pdf* neuropeptide gene mutation and ablation of PDF neurons each cause severe abnormalities of behavioral circadian rhythms in *Drosophila*. Cell *99*, 791–802.

Ruben, M., Drapeau, M.D., Mizrak, D., and Blau, J. (2012). A mechanism for circadian control of pacemaker neuron excitability. J. Biol. Rhythms *27*, 353–364.

Schmidt, A., and Hall, A. (2002). Guanine nucleotide exchange factors for Rho GTPases: turning on the switch. Genes Dev. *16*, 1587–1609.

Simões, S., Denholm, B., Azevedo, D., Sotillos, S., Martin, P., Skaer, H., Hombría, J.C., and Jacinto, A. (2006). Compartmentalisation of Rho regulators directs cell invagination during tissue morphogenesis. Development *133*, 4257–4267.

Sivachenko, A., Li, Y., Abruzzi, K.C., and Rosbash, M. (2013). The transcription factor Mef2 links the *Drosophila* core clock to Fas2, neuronal morphology, and circadian behavior. Neuron *79*, 281–292.

Stoleru, D., Peng, Y., Agosto, J., and Rosbash, M. (2004). Coupled oscillators control morning and evening locomotor behaviour of *Drosophila*. Nature *431*, 862–868.

Stoleru, D., Peng, Y., Nawathean, P., and Rosbash, M. (2005). A resetting signal between *Drosophila* pacemakers synchronizes morning and evening activity. Nature *438*, 238–242.

Stoleru, D., Nawathean, P., Fernández, M.P., Menet, J.S., Ceriani, M.F., and Rosbash, M. (2007). The *Drosophila* circadian network is a seasonal timer. Cell *129*, 207–219.

Van Aelst, L., and D'Souza-Schorey, C. (1997). Rho GTPases and signaling networks. Genes Dev. *11*, 2295–2322.

Veeman, M.T., and Smith, W.C. (2013). Whole-organ cell shape analysis reveals the developmental basis of ascidian notochord taper. Dev. Biol. *373*, 281–289.

Yao, Z., and Shafer, O.T. (2014). The *Drosophila* circadian clock is a variably coupled network of multiple peptidergic units. Science *343*, 1516–1520.

Yasuyama, K., and Meinertzhagen, I.A. (2010). Synaptic connections of PDF-immunoreactive lateral neurons projecting to the dorsal protocerebrum of *Drosophila melanogaster*. J. Comp. Neurol. *518*, 292–304.

Yoshii, T., Wülbeck, C., Sehadova, H., Veleri, S., Bichler, D., Stanewsky, R., and Helfrich-Förster, C. (2009). The neuropeptide Pigment-dispersing factor adjusts period and phase of *Drosophila*'s clock. J. Neurosci. *29*, 2597–2610.

Yu, W., and Hardin, P.E. (2006). Circadian oscillators of *Drosophila* and mammals. J. Cell Sci. *119*, 4793–4795.

Yuan, Q., Xiang, Y., Yan, Z., Han, C., Jan, L.Y., and Jan, Y.N. (2011). Light-induced structural and functional plasticity in *Drosophila* larval visual system. Science *333*, 1458–1462.

Zelinski, E.L., Deibel, S.H., and McDonald, R.J. (2014). The trouble with circadian clock dysfunction: multiple deleterious effects on the brain and body. Neurosci. Biobehav. Rev. *40*, 80–101.

Zhang, L., Chung, B.Y., Lear, B.C., Kilman, V.L., Liu, Y., Mahesh, G., Meissner, R.A., Hardin, P.E., and Allada, R. (2010). DN1p circadian neurons coordinate acute light and PDF inputs to produce robust daily behavior in *Drosophila*. Curr. Biol. *20*, 591–599.